Metallogeny and its link to orogenic style during the Nuna supercontinent cycle

SALLY J. PEHRSSON[1]*, BRUCE M. EGLINGTON[2], DAVID A. D. EVANS[3], DAVID HUSTON[4] & STEVEN M. REDDY[5]

[1]*Geological Survey of Canada, 601 Booth Street, Ottawa, Ontario, Canada K1A 0E8*

[2]*University of Saskatchwan, 114 Science Place, Saskatoon, Saskatchewan, Canada S7N 5E2*

[3]*Yale University, 210 Whitney Avenue, New Haven CT 06520–8109, USA*

[4]*Geoscience Australia, GPO Box 378 Canberra ACT 2601 Australia*

[5]*The Institute for Geoscience Research, Dept. of Applied Geology, Curtin University, GPO Box U1987, Perth WA6845, Australia*

**Corresponding author (e-mail: Pehrsson@nrcan.gc.ca)*

Abstract: The link between observed episodicity in ore deposit formation and preservation and the supercontinent cycle is well established, but this general framework has not, however, been able to explain a lack of deposits associated with some accretionary orogens during specific periods of Earth history. Here we show that there are intriguing correlations between styles of orogenesis and specific mineral deposit types, in the context of the Nuna supercontinent cycle. Using animated global reconstructions of Nuna's assembly and initial breakup, and integrating extensive databases of mineral deposits, stratigraphy, geochronology and palaeomagnetism we are able to assess spatial patterns of deposit formation and preservation. We find that lode gold, volcanic-hosted-massive-sulphide and nickel–copper deposits peak during closure of Nuna's interior ocean but decline during subsequent peripheral orogenesis, suggesting that accretionary style is also important. Deposits such as intrusion-related gold, carbonate-hosted lead-zinc and unconformity uranium deposits are associated with the post-assembly, peripheral orogenic phase. These observations imply that the use of plate reconstructions to assess orogenic style, although challenging for the Precambrian, can be a powerful tool for mineral exploration targeting.

Supplementary material: Supplementary material including (1) tables (S1–S3) of Euler poles and palaeopoles used, summary of Nuna orogens; (2) a figure (S1) of modelled plate velocities; (3) mp4 files (S1 & S2) of the model with age data; ore deposits and VGPs; and (4) a zip file (S1) of the Gplates model is available at http://www.geolsoc.org.uk/SUP18822.

Although Wegener (1912) successfully reconstructed, to first order, the Pangaea supercontinent almost exactly 100 years ago, attempts to reconstruct earlier, Precambrian landmasses are hampered by oceanic lithosphere subduction, poor biogeographic control, crustal recycling and erosion and palaeomagnetic overprinting. Neoproterozoic Rodinia has begun to take form (Li *et al.* 2008), evolving in a manner that appears consistent with Pangaean dynamics (Li & Zhong 2009). Palaeoproterozoic Nuna (also called Hudsonland or Columbia; Meert 2012; Evans 2013) reconstructions have suffered from inaccurate geometric rendering (Rogers & Santosh 2002; Zhao *et al.* 2002), merely regional palaeomagnetic consideration (Bispo-Santos *et al.* 2008; Hou *et al.* 2008) or lack of a coherent plate kinematic evolution (Hoffman 1997; Meert 2002; Pesonen *et al.* 2003; Payne *et al.* 2009). Recent models that do incorporate geometric accuracy and kinematic evolution are important first steps in a new approach to reconstruction (Evans & Mitchell 2011; Zhang *et al.* 2012). Further confidence in reconstructions can be gained from integrating global stratigraphic and geochronological information (Eglington *et al.* 2009; Pisarevsky *et al.* 2014), more routine usage of palaeomagnetic field stability tests to demonstrate primary ages of remanence (Buchan *et al.* 2000; Evans & Pisarevsky 2008) and innovative visualization software (Williams *et al.* 2012).

The use of palaeogeographical reconstructions in metallogenic targeting and understanding ore deposit controls has been hitherto limited for the Precambrian because of the inherent geometric and kinematic uncertainty of most reconstruction models. The aforementioned advances in Nuna models can now be viewed in the context of well-established linkages between the supercontinent

From: Li, Z. X., Evans, D. A. D. & Murphy, J. B. (eds) 2016. *Supercontinent Cycles Through Earth History*. Geological Society, London, Special Publications, **424**, 83–94.
First published online June 4, 2015, updated July 1, 2015, http://doi.org/10.1144/SP424.5

cycle and secular changes in ore deposit patterns (Barley & Groves 1992; Goldfarb *et al.* 2009; Cawood & Hawkesworth 2015) and specific deposit types recognized as associated with (a) continental assembly, for example, lode gold (Goldfarb *et al.* 2009), volcanic-hosted-massive sulphide (Huston *et al.* 2010) and carbonate-hosted lead–zinc (Leach *et al.* 2010) or (b) continental breakup, e.g. iron-oxide–copper–gold (IOCG; Groves *et al.* 2010) and sedimented-hosted copper (Hitzman *et al.* 2010). We present herein new intriguing observations about patterns of orogenesis and mineral deposit types, founded on the integration of extensive mineral deposit, geochronologic, stratigraphic and palaeomagnetic databases with a new animated, kinematically viable model for the assembly and breakup of Nuna. Our new model was developed and visualized utilizing PaleoGIS™ and GPlates (Williams *et al.* 2012) software, and enables assessment of patterns of mineralization within the supercontinent cycle. Although we do not consider it to be the last word on Nuna's evolution, we present the approach as an example of how a more dynamic process of reconstruction, robustly integrating multiple datasets, can bring about innovation.

Method and approach

Numerous reconstructions for an assembled Nuna, founded on palaeomagnetic (Rogers & Santosh 2002; Evans & Mitchell 2011; Zhang *et al.* 2012) or geological (Bispo-Santos *et al.* 2008; Meert 2002; Pesonen *et al.* 2003) data, or their combination (Pisarevsky *et al.* 2014), show a remarkable overall conformity. The current generation of Nuna models is loosely connected to the eventual assembly of a standard Rodinia model (Li *et al.* 2008) with minimal intervening motion. Relative placement of Laurentia with Baltica to its east (present coordinates) and Siberia to its north is common to all models, with minor variations in tightness of the Siberia–Laurentia connection (Pisarevsky *et al.* 2014). We follow recent reconstructions favouring a tighter fit (Evans & Mitchell 2011; Zhang *et al.* 2012). It is now standard to show Laurentia–Australia–Antarctica in a proto-SWEAT connection (Payne *et al.* 2009; Zhang *et al.* 2012) with Australia adjacent to northwestern Laurentia. Amazonia and West Africa are typically shown attached to Baltica (known as the SAMBA juxtaposition; Johansson 2009; Zhang *et al.* 2012), which we follow here because of minimal rearrangement forward in time to the standard Rodinia reconstruction. An alternative reconstruction positioning Amazonia–West Africa outboard of a peripheral subduction system on Laurentia's southern margin, and corollary of India adjacent to Sarmatia (Pisarevsky *et al.* 2014), faces greater difficulty in evolving towards Rodinia (Evans 2013). Kalahari may have been a lone craton, and Cathaysia is typically placed in the Australian sector (Li *et al.* 2008). Other cratons with differing locations in recent models include North China and India, which vary from clustered to separate in various positions (Zhao *et al.* 2002; Bispo-Santos *et al.* 2008; Hou *et al.* 2008; Evans & Mitchell 2011; Zhang *et al.* 2012). Our new model, utilizing PaleoGIS™ and GPlates (Williams *et al.* 2012) software, is presented as both an animation (see Supplementary material) and as five time slices through the interval 2.2–1.3 Ga (Figs 1–3), with known ore deposits superimposed. For this contribution we compiled more than 106 000 crystallization, metamorphism, cooling, summary detrital and model ages and more than 15 000 mineralization occurrences with deposit types in the StratDB and Dateview databases (publically available online from http://sil.usask.ca/databases.htm). Most deposit information was compiled and modified from the World Mineral Deposit database of the Geological Survey of Canada. Particular care was taken to integrate digital map-based craton topologies, relative positions and convergence of cratons linked with orogenic history, and avoid overlap of cratons following convergence. We created 678 plate polygons in ArcGIS™ based on digital geological and geophysical maps, refined by information from the above databases and the literature (Supplementary Document S1 and Supplementary Model S1 in the Supplementary material). Deposit and geochronological point locality information and attributes were linked to the plates via a spatial join in ArcMap™.

The model was developed using GPlates (http://www.gplates.org), PaleoGIS (http://www.Paleogis.com) and custom-developed software, assuming rigid plates throughout. Our continuous GPlates™ model of Nuna evolution from 2.2 to 1.3 Ga is presented in a series of time steps (Supplementary animations S1 and S2 and Supplementary Model S1 in the Supplementary material) and is based on orogen histories (Supplementary Table S1 and vergence, geometry, viable plate velocities and palaeomagnetic data, the latter a subset of highest-reliability poles from a comprehensive and rigorous assessment of the global palaeomagnetic database (Supplementary Table S2). Validity of the model was tested through comparison of virtual geomagnetic poles for reconstructed plates and integration of known orogens (Supplementary Movie S2 and Table S2), together with acceptable geometric relationships for plate motions, patterns in geochronology and for geology. The Supplementary Movie S1 shows our reconstruction at 1 Ma time steps, together with virtual geomagnetic poles for cratons with palaeomagnetic control. Supplementary Movie

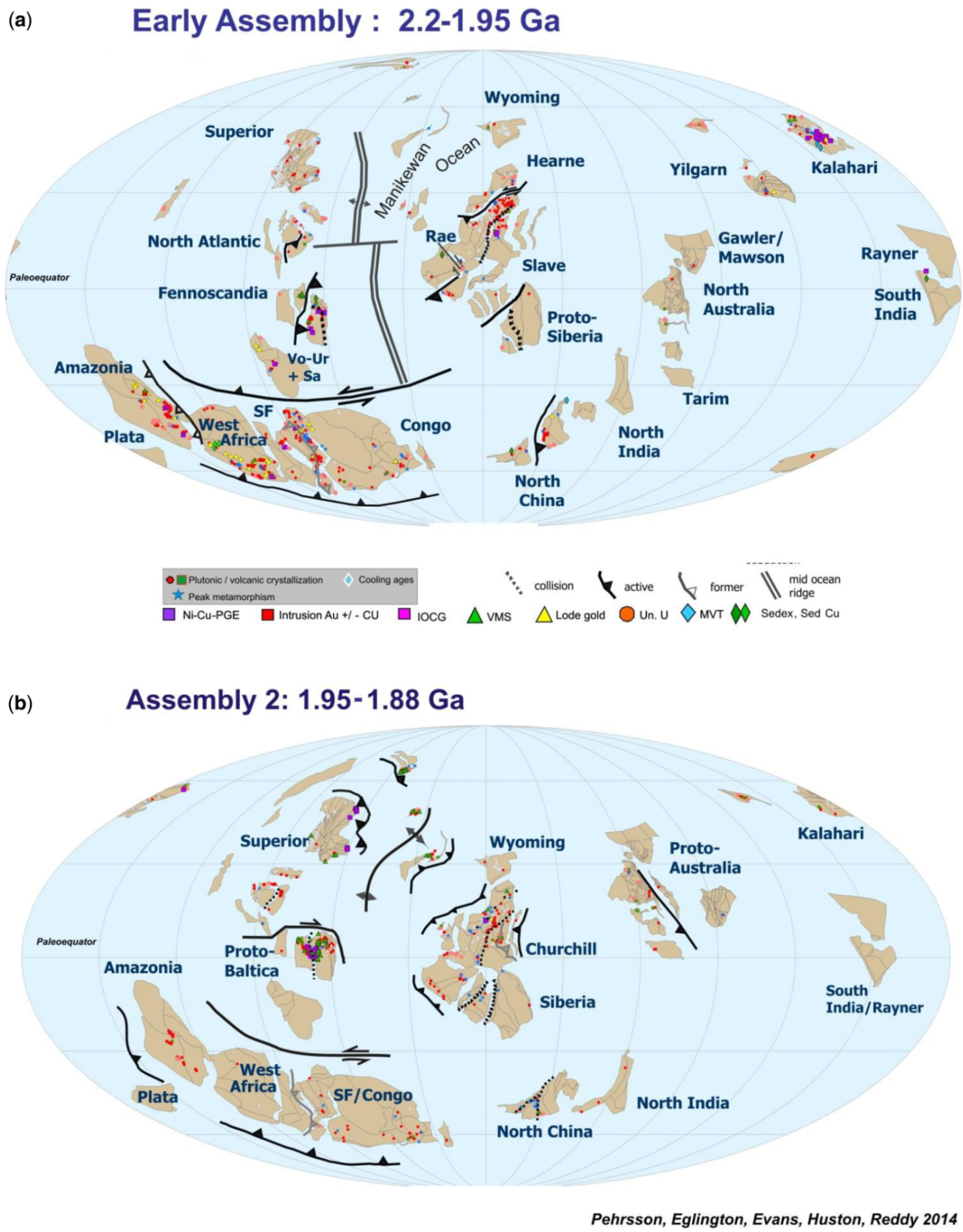

Fig. 1. Timeslices of Nuna reconstruction during early assembly. (**a**) Reconstruction for the period 2.2–1.95 Ga. (**b**) Reconstruction for the period 1.95–1.88 Ga. Coloured symbols plotted on plates represent crystallization data (small dots), tectonometamorphism data (blue stars) and ore deposits (large symbols) occurring at times throughout the age range. The grey dotted and dashed lines denote sites of collision and former subduction respectively in the time range. Not all possible such zones are ornamented for clarity, only the major systems. For sources of data see Supplementary datasets. Images produced using PaleoGIS^{TM}. Abbreviations as follows: Ca, Cathaysia; IOCG, iron-oxide–copper–gold; VMS, volcanic-hosted massive sulphide; Un. U, unconformity uranium; MVT, Mississippi Valley-type lead–zinc; Sedex, sedimentary exhalative Pb-Zn; Sed Cu, sediment-hosted copper. Discussed in text.

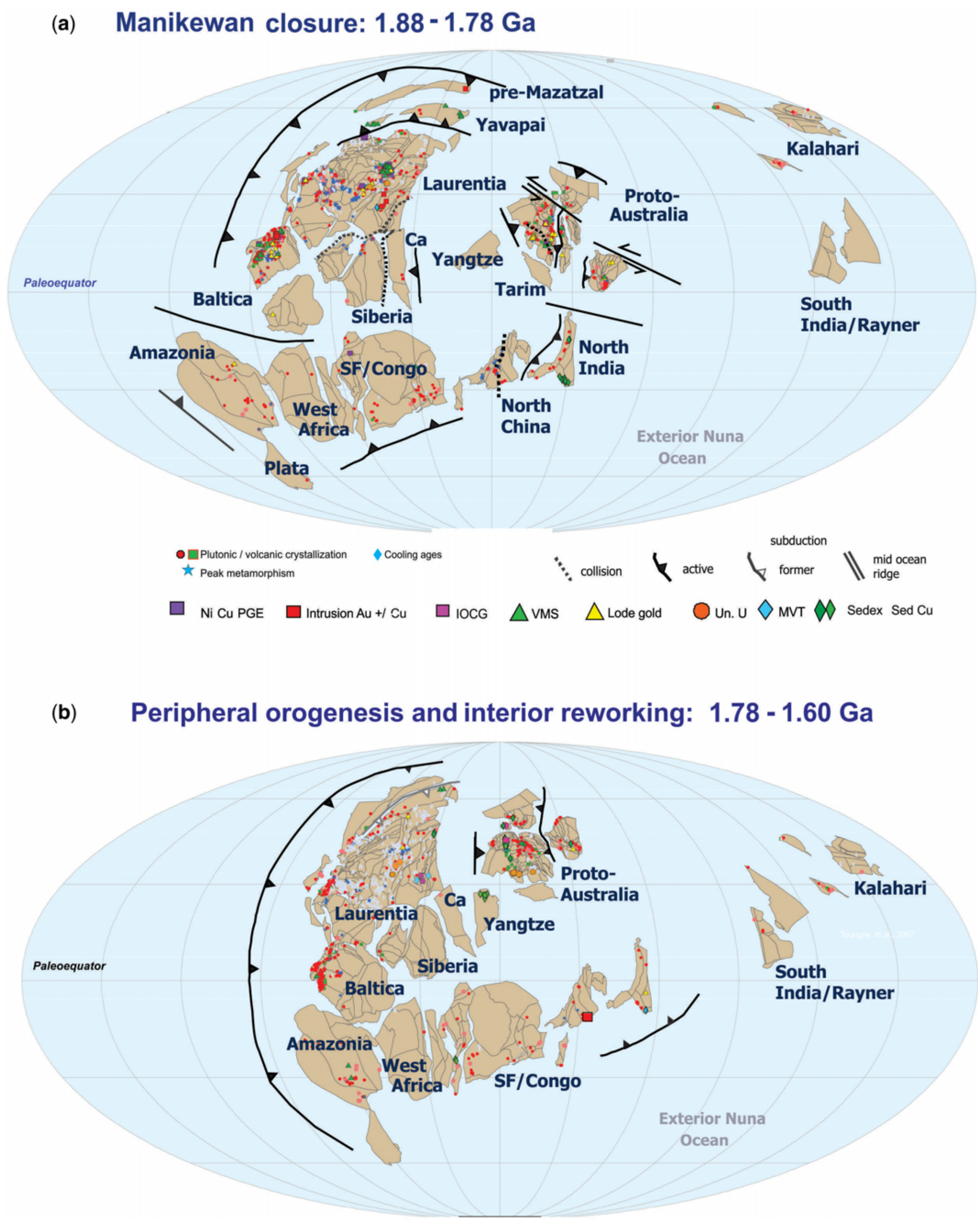

Fig. 2. Timeslices of Nuna reconstruction during late and final assembly. (**a**) Reconstruction for the period 1.88–1.78 Ga. (**b**) Reconstruction for the period 1.78–1.6 Ga. Abbreviations, symbols and ornamentation as in Figure 1. For sources of data see Supplementary datasets. Images produced using PaleoGIS^{TM}. Discussed in text.

S2 is an animated PaleoGIS^{TM}-generated movie showing Nuna evolution from 2.1 to 1.3 Ga in 5 Ma steps with the associated geochronology and mineral deposits shown. Supplementary Movie S1 illustrates the density and confluence of poles and Supplementary Figure S1 shows calculated plate speeds for the model, highlighting that, whereas some parts of the model are dominantly fitted

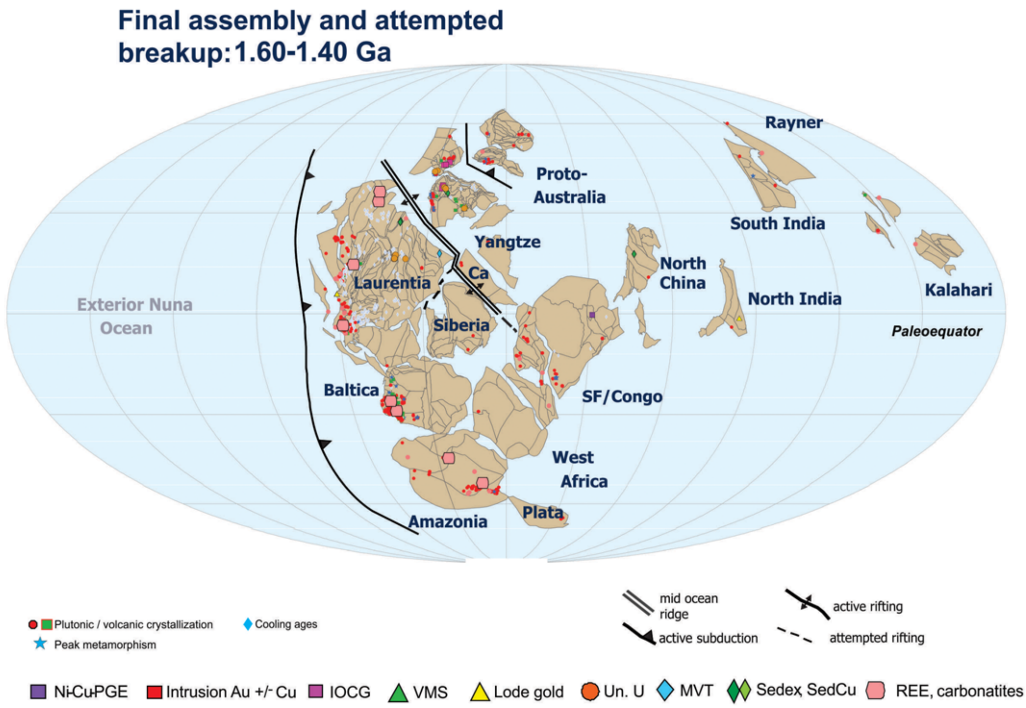

Fig. 3. Timeslice of Nuna reconstruction post-assembly. Abbreviations, symbols and ornamentation as in Figure 1. Reconstruction for the period 1.6–1.45 Ga illustrates ongoing peripheral magmatism after final assembly and localized magmatic–metallogenic events in the interior during initial breakup. For sources of data see Supplementary datasets. Images produced using PaleoGIS™. Discussed in text.

on geology, the model is nevertheless consistent in honouring plate velocities known from the Phanerozoic.

Absolute palaeolongitude of the Nuna centroid was defined assuming the orthoversion model of Mitchell *et al.* (2012), assuming approximate centroids for supercontinents at 800, 1500 and 2200 Ma. Palaeolongitude for individual blocks was distributed between the supercontinent extremes so as to honour palaeolatitude requirements, plate motion geometries and velocities while also striving to achieve kinematic realism. Individual plate assembly and orientation were further assessed using geology and deposit models, ensuring geodynamically realistic settings for syngenetic deposit types. Probability curves and cumulative frequency plots were produced with FitPDF (http://sil.usask.ca/software.htm) or from within the DateView web interface.

Kinematic uncertainty dominantly arises from inhomogeneity in the palaeomagnetic record in both time and space. Unavoidably, we cannot correct for lithosphere lost during subsequent breakup, shortening during younger compressional events or subduction erosion, which may have occupied some gaps between clusters of cratons. We deliberately maintain a looser fit between plates at this stage of model development so as to facilitate future improvements to the model without the need for major restructuring of the relative positions of multiple plates to accommodate small localized improvements.

Our final configuration follows that of Zhang *et al.* (2012) in most respects, although we have modified the position of India based on new data and show a later final assembly time of Nuna, according to recognition of tectonic mobilization throughout North Australia between 1.8 and 1.6 Ga (Cawood & Korsch 2008; Payne *et al.* 2009). We show Nuna undergoing extensional tectonic conditions as early as 1.5 Ga, but breaking up in earnest as late as 1.3 Ga, following Zhang *et al.* (2012). We note that there is significant agreement between this and current models discussed above, with dominantly minor variations involving cratons on Nuna's periphery. Although we expect models for Nuna evolution to evolve, we suggest that there is sufficient consilience about its overall makeup to allow the present evaluation of patterns of mineralization during its history.

Amalgamation and tenure of the Nuna supercontinent

Assembly of Nuna began slowly but accelerated with time, as evident in the punctuated, diachronous development of accretionary and collisional activity during 2.2–1.88 Ga (Fig. 1a, b). An early stage of 2.2–2.0 Ga accretionary orogenesis initially involved only six cratonic blocks focused in the nascent supercontinent's southern and eastern sectors (Fig. 1a; all directions refer to reconstruction coordinates shown in the figures), and built early constituent cratons including West Africa–Amazonia and Congo–São Francisco. This early accretion phase overlapped with ongoing expansion of the Manikewan ocean in the Northern Hemisphere, and proceeded diachronously northward with an increasing number of 2.0–1.95 Ga accretionary and collisional events in what later would become Baltica, Siberia, Laurentia and Greenland. Between 1.95 and 1.88 Ga, contraction of Manikewan and other seaways began and then accelerated, with accretion of various microcontinents to a growing Laurentian nucleus (Fig. 1b).

In a similar fashion, Nuna's southern and eastern sectors saw the internal assembly and convergence of Baltica and proto-Australia blocks, respectively. This distinct spatial progression and tempo of assembly is echoed by the global tectonometamorphic and magmatic record, which slows a clear early diachroneity, culminating in pan-Nuna events at *c.* 1.88 Ga (Fig. 4).

Collisional orogenesis related to Manikewan ocean closure and Nuna assembly dominated the period between 1.88 and 1.78 Ga (Fig. 2a). The early accretionary orogens associated with internal ocean closure were in what are now Laurentia, Siberia and Baltica. We propose that the essential framework of Nuna was largely complete by 1.85–1.8 Ga, as reflected in the bloom of tectonometamorphism at that time. In our model, Congo–São Francisco craton collided with newly amalgamated Siberia by *c.* 1.83 Ga to give rise to magmatism and thermal resetting known in Angola and locally in the São Francisco craton. Assembly of the various blocks comprising North China, southern India, and proto-North Australia, define a distinct cluster of rapid contraction in Nuna's eastern sector, and may have given rise to the voluminous late Palaeoproterozoic iron-formation belts (Bekker *et al.* 2010), owing to vigorous submarine hydrothermal venting during intraoceanic subduction. In our geometry, the youngest phases of Trans-Hudsonian orogenesis, at *c.* 1.80–1.78 Ga, are focused increasingly towards the periphery of a large completed sector of the core of Nuna. Subsequent events, highlighted by patterns of magmatism and metamorphism (Figs 2 & 3) are focused more outboard

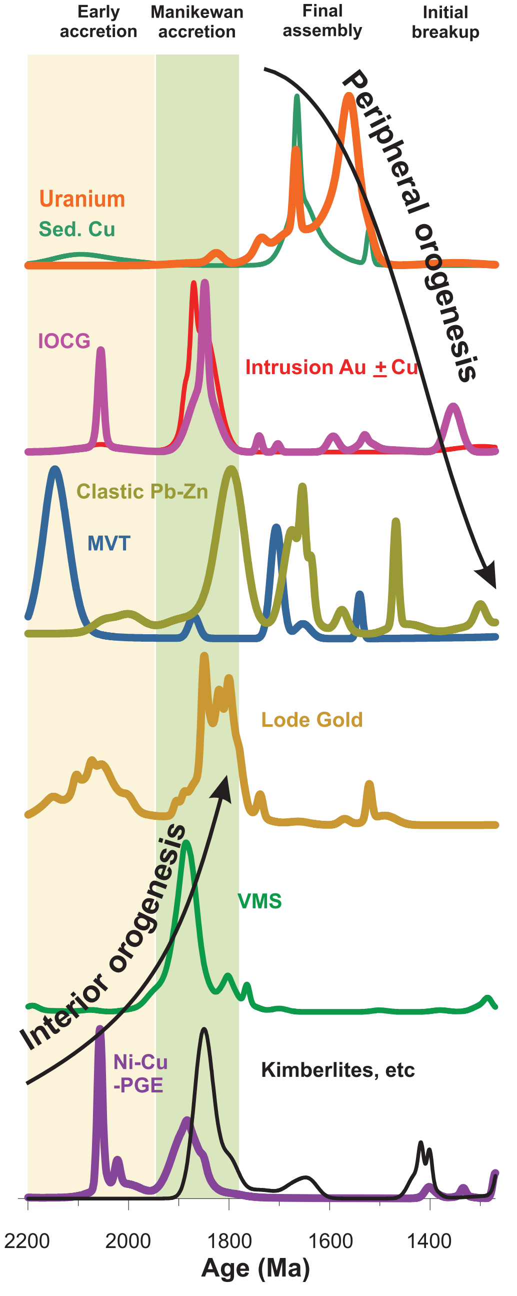

Fig. 4. Ore deposit classes and Nuna assembly phases. Probability curves of ore deposit classes through Nuna history. Height of peak represents relative probability of occurrence against total number of deposits for that individual deposit type. For sources of data see Supplementary datafile. Note the distinct change in types of deposits associated with the interior collisional and peripheral orogenic phases, suggesting that Ni–Cu–PGE, VMS and orogenic lode gold have less preservation potential in the latter phase.

including the Australia–China–India sector and adjacent regions of Laurentia.

Following terminal Manikewan convergence by 1.82 Ga (Fig. 2b), orogenic activity stepped out to what would become Nuna's long-lived convergent margins. In our model, the extensive northern and western peripheral orogenic belt (Mawson–Laurentia–Rockall–Greenland–Baltica–Amazonia) stabilized and transiently coupled with the interior, driving episodic events of far field compressional reactivation and local extension. The Australia–North China–India sector was active, with repeated alternating periods of compression, magmatism, rifting and intracratonic basin formation between 1.78 and 1.6 Ga, conceivable within an overall, north-facing retreating peripheral subduction setting (Fig. 2a). Ultimately, we propose that Australia accreted late in Nuna's history and was quickly separated by a narrow seaway that formed one arm of a triple junction between Laurentia–Siberia–Australia. This triple junction focused early attempted breakup of Nuna, contemporaneous with bimodal volcanism *c.* 1.75 and 1.66 Ga, the volcanomagmatic record of which is found throughout north-central Nuna, including Australia, Laurentia, Yangtze and North China (Fig. 2b).

A remnant ocean basin between North Australia and the west Laurentia sector accounts for (a) an active orogenic and magmatic history in North Australia at 1.7–1.6 Ga that is absent in west Laurentia, (b) palaeomagnetic evidence for locally rapid continental motion (Idnurm 2000) in North Australia but not Laurentia and (c) the presence of marine sedimentation and oceanic volcanism in western Laurentia and northeasternmost Australia. Our placement of Yangtze craton along-strike from North Australia at *c.* 1.7 Ga forms a plausible cluster of similarly aged sedimentary-hosted copper deposits in a sector with associated extensional–intracratonic sedimentation. Importantly, long-lived peripheral or retreating orogenic activity on the western and eastern margins of Nuna in our reconstruction may explain Bradley's (2008) observation that passive margins are at a minimum during this period in Earth history.

After 1.6 Ga the supercontinent drifted to more southerly palaeolatitudes (Fig. 3). Attempted but unsuccessful breakup events remained focused about the Laurentia–Australia–Siberia nexus, which kept the greater Nuna geometry intact to 1.4–1.3 Ga, when numerous mafic dyke swarms indicate extension in that central region (Hou *et al.* 2008). Superposition of the earlier extensional efforts (seen in the global record of rift basins, large igneous provinces, lamproites, kimberlites and metasomatic events) on the recently amalgamated supercontinent led to tapping of highly metasomatized subcontinental lithospheric mantle on a scale not previously seen, and formation of the globe's largest rapakivi and ultrapotassic magmatic provinces (Haapala & Ramo 1999; Peterson *et al.* 2010). Orogenic activity focused in the Australian sector drove indentation and reactivation in the more stable central core of Nuna, concomitant with deposition of the major late Palaeoproterozoic to early Mesoproterozoic intracontinental basins (Eglington *et al.* 2013). Ongoing peripheral orogenesis on the western (Amazonia–Baltica–Laurentia) margin caused transient magmatic flare-ups (the so-called granite–rhyolite event) and inversion of sedimentary basins (Bickford *et al.* 2010).

Integration of the ore deposit record and reconstruction

Patterns of mineralization corroborate the kinematic model presented in Figures 1–3. For example, deposit types that form in collisional or accretionary settings (i.e. orogenic lode-gold and volcanic-hosted massive sulphide, VMS), do not fall on passive margins, and deposits that tend to form in more equatorial latitudes (sedimentary and carbonate-hosted Pb–Zn and sediment-hosted copper; Leach *et al.* 2010; Groves *et al.* 2010) are consistent with our modelled palaeogeography. Comparison of the three main accretionary phases (2.2–1.95, 1.95–1.88 and 1.88–1.78 Ga) shows that only the third phase is associated with a global bloom in VMS, including the world-class Flin Flon, Skellefte and Outukumpu districts. This supports models that favour significant preservation of VMS deposits where accretion quickly follows formation in periods of rapid convergence (Huston *et al.* 2010). The earlier south to north progressive assembly of Nuna is similarly mirrored by a pattern of sequential preservation of VMS deposits followed by synorogenic lode gold mineralization shortly thereafter in recently accreted sequences (e.g. West Africa (Perkoa and Afema), Baltica (Boliden and Bjorkdal) and Laurentia (Flin Flon and New Britannia)).

Ultimately, closure of the Manikewan interior ocean led to clustering of numerous ore deposit types within Laurentia–Baltica, including orogenic lode gold, VMS, Kiruna-type and Great Bear-type IOCG deposits in late-stage continental arcs built on already amalgamated margins. During the later accretionary phases a unique overlap between secular trends in ocean-atmosphere chemistry and a local arc-backarc setting may have given rise to the 1.85–1.80 Ga clastic-hosted Pb–Zn Aravelli–Delhi district of India (Deb & Thorpe 2004).

Our integration of the global mineral deposit database with the reconstruction underscores the point that some types of deposits are predictive of tectonic setting and can be used to constrain reconstructions. Huston *et al.* (2010) have noted the nearly complete lack of VMS and lode gold deposits in northeastern Australia after 1.7 Ga, suggesting that this is consistant with a dominantly extensional setting. In our model the locus of sediment-hosted copper deposits in that sector (Australia, Yangtze) is also supportive of an extensional setting, given the interpreted tectonic setting for their formation (Hitzman *et al.* 2010). In a similar manner we suggest that the lack of Chinese Palaeoproterozoic lode gold and VMS deposits at this time, deposits that form in convergent settings (Groves *et al.* 2005; see also Huston *et al.* 2012), qualitatively supports our placement of it in a more peripheral setting. The integrated reconstruction approach shown here can also ultimately lead to a reassessment of deposit ages. Lode gold deposits in Siberia and North China, long considered early Mesoproterozoic in established databases (Dubé & Gosselin 2007), but situated implausibly inboard and dated as substantially post-accretion, may actually be Phanerozoic (Xiaohui *et al.* 2005).

The new palaeogeography also has major implications for existing deposit models. We note a tendency for the great Mesoproterozoic unconformity uranium deposits to fall along a palaeolatitudinal band limited to the subtropics (Fig. 3), which is intriguing given recent evidence for involvement of evaporative brines in deposit formation (Mercadier *et al.* 2011). The lack of unconformity uranium mineralization in the Amazonia–West Africa–Congo sector after 1.7 Ga, despite deposition of suitable sequences, could then be explained by the supercontinent's drift and latitudinal position, which placed this sector in higher southerly palaeolatitudes unfavourable for formation of an evaporative brine factory. If correct, our model highlights the predictive power of stratigraphy and reconstructions for targeting uranium in global Mesoproterozoic basins.

Nuna's assembly and ore deposit record (Fig. 4) supports new models for Ni–Cu–platinum group element (PGE) potential in large igneous provinces. Begg *et al.* (2010) have noted the tendency for Ni–Cu–PGE deposits to form in such provinces near cratonic margins during periods of active regional tectonism, most commonly under compressional to transpressional conditions. In our model the globally important 1.9–1.88 Ga spike in Ni–Cu–PGE mineralization (Naldrett 2010) and large igneous province formation are contemporaneous with the period of accelerated closure of the Manikewan interior ocean (Fig. 5), intraoceanic accretion and the major peak of VMS mineralization (Fig. 4). This temporal overlap suggests that both deposit types are favoured by localized extension within an overall contractional system (Huston *et al.* 2010; Naldrett 2010) related to shortening of the abundant pericratonic arcs and related marginal basins distributed about the cratonic margins of the contracting juvenile ocean. The conceptual model that deposits are smaller where associated with sites of possible lithospheric delamination following accretion (Begg *et al.* 2010) as opposed to mantle plume melting also holds for Nuna, particularly for *c.* 1.87–1.85 Ga deposits of Laurentia.

A relative paucity of Ni–Cu–PGE deposits is noted in the interval 1.8–1.4 Ga despite a reasonable abundance of mafic magmatism (Ernst *et al.* 2008). Focused introduction of mantle plume-related high-degree melts into the crust at craton margins, a factor most favoured by relatively compressional/transpressional tectonic conditions about Nuna's periphery, is considered optimal for the formation of these deposits (Begg *et al.* 2010). The more intracratonic-focused mafic magmatism between 1.6 and 1.4 Ga may be due to relatively low-degree mantle melting associated with repeated failed breakup events prior to interpreted eventual incomplete breakup of Nuna ca 1.27 Ga (Evans & Mitchell 2011, and references therein). We suggest that the paucity of observed Ni–Cu–PGE deposits prior to 1.4 Ga, relates to a relative low in mantle plume activity coupled with overall relatively unfocused extensional tectonic conditions at this time. The major deposit known in this time period, Kabanga in the Congo craton (Maier *et al.* 2010, fig. 3), we suggest relates to a failed rift near the tectonically active periphery. The increased abundance of Mesoproterozoic Ni–Cu–PGE deposits from 1.4–1.0 Ga fits with our interpretation that Nuna did not ultimately break up until after 1.4 Ga (Evans & Mitchell 2011), when mantle-plume activity increased.

Patterns of metallogeny in supercontinent assembly

A systematic shift in type and frequency of deposit formation/preservation is noted during the Nuna supercontinent cycle (Fig. 4). The diachronous interior ocean-closure phase resulted in an overlap between contraction-related deposits (VMS, lode gold and Ni–Cu–PGE) and some magmatic-related deposit types (porphyry Cu–Au and some types of IOCG). Following the switch to peripheral orogenesis after assembly, the volume of VMS, lode gold and Ni–Cu–PGE deposits dropped dramatically, despite ongoing active subduction, magmatism and orogenesis (Figs 2b, 3 & 4), conditions that might seem favourable for their formation. The peripheral orogenic phase is instead associated with a bloom of either extension-related deposits during attempted breakup periods (sedimentary-Cu, clastic Pb–Zn

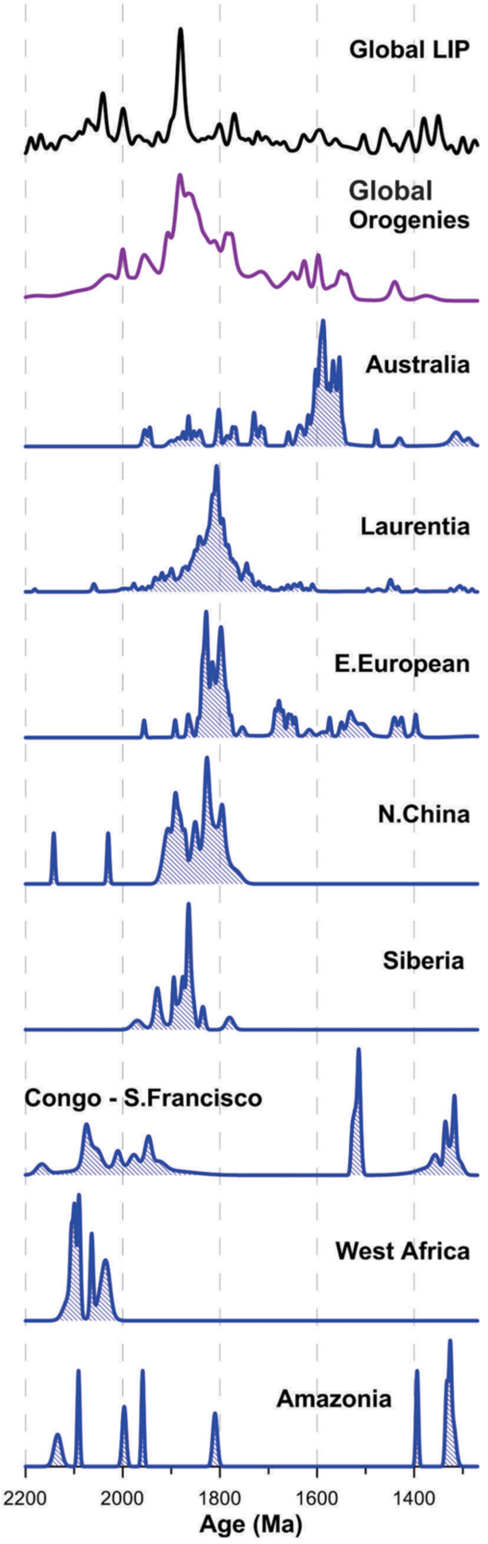

Fig. 5. Temporal patterns of Nuna orogenesis and large igneous province events. Cumulative frequency plot of compiled orogenic events (igneous events (blue) and metamorphism (purple)) for selected individual cratons and large igneous province events during Nuna evolution between 2200 and 1270 Ma. Plotted with Gaussian frequency distribution 'AND'. As noted in text, Nuna accretionary orogenesis started slowly but quickly peaked *c.* 1880 Ma. The systematic temporal shift with progressive northward amalgamation is evident prior to *c.* 1880 Ma. Punctuated magmatic and metamorphic events in the Mesoproterozoic attest to the long-lived peripheral margin. For sources of data see Supplementary datasets.

and IOCG) or deposits formed where peripheral orogenesis directly affects favourable stratigraphic hosts (Mississippi Valley-type lead–zinc) or triggers interior reactivation of intracontinental basins (unconformity uranium) (Jefferson *et al.* 2007). We suggest that the repeated attempted late Palaeoproterozoic–Mesoproterozoic breakup events actively moved metals and fluids from the fertilized subcontinental lithospheric mantle (via low-degree partial melts) to the upper crust (Hopp *et al.* 2008; Lazarov *et al.* 2009; Peterson *et al.* 2010; Griffin *et al.* 2013), where they were available be scavenged into the world-class IOCG (Olympic Dam) and unconformity uranium (Athabasca–Kombolgie) districts.

A trend towards a lack of preservation of contraction-related deposits in the peripheral orogenic phase may explain some unusual secular trends. The paucity of carbonate-hosted Pb–Zn deposits in general during Nuna evolution may be explained by its early internal evolution, in which there appears to be a lack of long-enduring, stable passive margins, a situation further exacerbated by a lack of overprinting orogenesis in suitable palaeolatitudes (Eglington *et al.* 2013). Researchers have noted the absence of peaks in juvenile crust formation (Condie 1998) and ore deposit preservation (Meyer 1981; Groves *et al.* 2005) during Rodinia assembly, at odds with predicted increased preservation during supercontinent assembly (Barley & Groves 1992). Our model predicts that Rodinia should have less metal endowment, owing to its evolution as a supercontinent formed by closure of long-lived peripheral orogens (Li *et al.* 2008), largely inherited from Nuna and involving large tectonic plates from Nuna's incomplete breakup. We suggest that supercontinents in which there is relatively little deposit endowment and juvenile crustal addition, but known spikes in zircon formation (Belousova *et al.* 2010) like Rodinia, will have formed by dominantly advancing accretionary orogenesis in peripheral orogens that doomed direct preservation of contraction-related deposits and related magmatic rocks. Whether the lack of contraction-related deposits in the peripheral orogenic phase is a result of a lack of preservation owing to post-orogenic erosion or to simply a lack of formation remains to be studied.

Future approach

The animated reconstruction approach outlined here can be used as a platform for evaluation of all systems linked to supercontinent formation and breakup, including mineralizing, atmospheric–hydrospheric and geodynamic settings. We suggest that, although this preliminary model will be refined as more data and regional geological constraints become available, in future all reconstructions will benefit from integration of deposit endowment, bringing a more holistic yet quantitative approach to assessments of Earth evolution. Conversely, we hope to expand the deposit types included and refine deposit classifications, drivers and geodynamic settings based on tightly constrained younger reconstructions, with the aim of informing exploration models. Ultimately, such improved animated reconstructions could serve as preliminary reference models for many other avenues of research, including climate simulation, secular evolution of the atmosphere and hydrosphere, and biological development through Earth's 'middle age' (Reddy & Evans 2009).

Author contributions

S.P. and B.E developed the conceptual idea for the study. B.E., S.R. and D.E. designed and developed the databases. B.E. compiled geochronology data and developed the web interfaces and the digital representation of the datasets; B.E., S.P. and D.E. developed the plate model; S.P., D.H. and B.E. compiled ore deposit information in the databases; S.P. and B.E. compiled the orogen summary and kinematics; D.E. compiled and assessed the palaeomagnetic data; all authors contributed to discussions and writing of the manuscript.

This work arose from the UNESCO IGCP project 509. S.P.'s work has been a contribution to the Geological Survey of Canada's Targeted Geoscience Initiative-3 and Geoscience for Energy and Minerals programs. B.E. acknowledges an NSERC Discovery grant. Rothwell Group provided PaleoGIS software used for the reconstructions. The authors are grateful for discussions with F. Alkmim, A. Bekker, B. Collins, C. Jefferson and R. Rainbird and a particularly thorough and helpful earlier review by G. Begg. Geological Survey of Canada contribution no. 20130034.

References

Barley, M. E. & Groves, D. I. 1992. Supercontinent cycles and the distribution of metal deposits through time. *Geology*, **20**, 291–294.

Begg, G. C., Hronsky, J. A. M., Arndt, N. T., Griffin, W. L., O'Reilly, S. Y. & Hayward, N. 2010. Lithospheric, Cratonic, and Geodynamic Setting of Ni–Cu–PGE Sulfide Deposits. *Economic Geology*, **105**, 1057–1070.

Bekker, A., Slack, J. F. *et al.* 2010. Iron formation: the sedimentary product of a complex interplay among mantle, tectonic, oceanic, and biospheric processes. *Economic Geology*, **105**, 467–508.

Belousova, E. A., Kostitsyn, Y. A., Griffin, W. L., Begg, G. C., O'Reilly, S. Y. & Pearson, N. J. 2010. The growth of the continental crust: constraints from zircon Hf-isotope data. *Lithos*, **119**, 457–466.

Bickford, M. E., Karlstrom, K. E. *et al.* 2010. Early Mesoproterozoic (1.5–1.3 Ga) magmatic and tectonic evolution of the SE Laurentian cratonic margin; implications of U–Pb, Sm–Nd, and Lu–Hf data. *In*: *Geological Society of America, North-Central Section, 44th Annual Meeting and Geological Society of America, South-Central Section, 44th Annual Meeting Abstracts with Programs*. Geological Society of America, Boulder, CO, **42**, 47.

Bispo-Santos, F., D'Agrella-Filho, M. S. *et al.* 2008. Columbia revisited; paleomagnetic results from the 1790 Ma Colider volcanics (SW Amazonian Craton, Brazil). *Precambrian Research*, **164**, 40–49.

Bradley, D. C. 2008. Passive margins through earth history. *Earth Science Reviews*, **91**, 1–26.

Buchan, K. L., Mertanen, S. *et al.* 2000. Comparing the drift of Laurentia and Baltica in the Proterozoic: the importance of key palaeomagnetic poles. *Tectonophysics*, **319**, 167–198.

Cawood, P. A. & Hawkesworth, C. J. 2015. Temporal relations between mineral deposits and global tectonic cycles: implications for prospectivity. *In*: Jenkin, G. R. T., Lusty, P. A. J., McDonald, I., Smith, M. P., Boyce, A. J. & Wilkinson, J. J. (eds) *Ore Deposits in an Evolving Earth*. Geological Society, London, Special Publications, **393**, 9–21.

Cawood, P. A. & Korsch, R. 2008. Assembling Australia: proterozoic building of a continent. *Precambrian Research*, **166**, 1–38.

Condie, K. C. 1998. Episodic continental growth and supercontinents: a mantle avalanche connection? *Earth and Planetary Science Letters*, **163**, 97–108.

Deb, M. & Thorpe, R. I. 2004. Geochronological constraints in the Precambrian geology of Rajasthan and their metallogenic implications. *In*: Deb, M. & Goodfellow, W. D. (eds) *Sediment-Hosted Lead–Zinc Sulphide Deposits*. Narosa Publishing House, New Delhi, 246–263.

Dubé, B. & Gosselin, P. 2007. Greenstone-hosted quartz–carbonate vein deposits. *In*: Goodfellow, W. D. (ed.) *Mineral Deposits of Canada: A Synthesis of Major Deposit-Types, District Metallogeny, the Evolution of Geological Provinces, and Exploration Methods*. Geological Association of Canada Mineral Deposits Division, Ottawa, Canada, Special Publications, **5**, 49–73.

Eglington, B. M., Reddy, S. M. & Evans, D. A. D. 2009. The IGCP 509 database system: design and application of a tool to capture and illustrate litho- and chrono-stratigraphic information for Palaeoproterozoic tectonic domains, large igneous provinces and ore deposits; with examples from southern Africa. *In*: Reddy, S. M., Mazumder, R. & Evans, D. A. D. (eds) *Palaeoproterozoic Supercontinents and Global Evolution*. Geological Society, London, Special Publications, **323**, 27–47.

Eglington, B. M., Pehrsson, S. J. *et al.* 2013. A domain-based digital summary of the lithostratigraphy, geochronology and geodynamics of the Palaeoproterozoic of North America and Greenland and associated unconformity-type uranium mineralization. *Precambrian Research*, **232**, 4–26.

Ernst, R. E., Wingate, M. T. D., Buchan, K. L. & Li, Z.-X. 2008. Global record of 1600–700 Ma Large Igneous Provinces (LIPs): implications for the reconstruction of the proposed Nuna (Columbia) and Rodinia supercontinents. *Precambrian Research*, **160**, 159–178.

Evans, D. A. D. 2013. Reconstructing pre-Pangean supercontinents. *Geological Society of America Bulletin*, **125**, 1735–1753.

Evans, D. A. D. & Mitchell, R. N. 2011. Assembly and breakup of the core of Paleoproterozoic–Mesoproterozoic supercontinent Nuna. *Geology*, **39**, 443–446.

Evans, D. A. D. & Pisarevsky, S. A. 2008. Plate tectonics on early Earth? Weighing the paleomagnetic evidence. *In*: Condie, K. C. & Pease, V. (eds) *When Did Plate Tectonics Begin on Planet Earth?* Geological Society of America, Boulder, CO, Special Papers, **440**, 249–263.

Goldfarb, R. J., Groves, D. I., Kerrich, R. & Leach, D. L. 2009. Metallogenic evolution on an evolving Earth. *In*: *Proceedings of the Tenth Bienniel SGA Meeting*, *Townsville, Australia*, 11–13.

Griffin, W. L., Begg, G. C. & O'Reilly, S. Y. 2013. Continental-root control on the genesis of magmatic ore deposits. *Nature Geoscience*, **6**, 905–910.

Groves, D., Bierlein, F. P., Meinert, L. D. & Hitzman, M. W. 2010. Iron oxide copper–gold (IOCG) deposits through Earth history: implications for origin, Lithospheric Setting, and distinction from other epigenetic iron oxide deposits. *Economic Geology*, **105**, 641–654.

Groves, D. I., Vielreicher, R. M., Goldfarb, R. J. & Condie, K. C. 2005. Controls on the heterogeneous distribution of mineral deposits through time. *In*: McDonald, I., Boyce, A. J., Butler, I. B., Herrington, R. J. & Polya, D. A. (eds) *Mineral Deposits and Earth Evolution*. Geological Society, London, Special Publications, **248**, 71–101.

Haapala, I. & Ramo, O. T. 1999. Rapakivi granites and related rocks: an introduction. *Precambrian Research*, **95**, 1–7.

Hitzman, M. W., Selley, D. & Bull, S. 2010. Formation of sedimentary rock-hosted stratiform copper deposits through earth history. *Economic Geology*, **105**, 627–639.

Hoffman, P. F. 1997. Tectonic genealogy of North America. *In*: Van der Pluijm, B. A. & Marshak, S. (eds) *Earth Structure: An Introduction to Structural Geology and Tectonics*. McGraw-Hill, New York, 459–464.

Hopp, J., Trieloff, M., Brey, G. P. & Woodland, A. B. 2008. $^{40}Ar/^{39}Ar$ ages of phlogopite in mantle xenoliths from South Afican kimberlites; evidence for metasomatic mantle impregnation during the Kibaran orogenic cycle. *Lithos*, **106**, 351–364.

Hou, G., Santosh, M., Qian, X., Lister, G. S. & Li, J. 2008. Configuration of the Late Paleoproterozoic supercontinent Columbia: insights from radiating mafic dyke swarms. *Gondwana Research*, **14**, 395–409.

Huston, D. L., Pehrsson, S. J., Eglington, B. M. & Zaw, K. 2010. The geology and metallogeny of volcanic-hosted massive sulfide deposits: variations through geologic time and with tectonic setting. *Economic Geology*, **105**, 571–591.

Huston, D. L., Blewett, R. S. & Champion, D. C. 2012. Australia through time: a summary of its tectonic and metallogenic evolution. *Episodes*, **35**, 23–43.

Idnurm, M. 2000. Toward a high resolution Late Palaeoproterozoic–earliest Mesoproterozoic apparent polar wander path for northern Australia. *Australian Journal of Earth Science*, **47**, 405–430.

Jefferson, C. W., Thomas, D. J. *et al.* 2007. Unconformity associated uranium deposits of the Athabasca Basin, Saskatchewan and Alberta. *In*: Jefferson, C. W. & Delaney, G. (eds) *EXTECH IV: Geology and Uranium Exploration Technology of the Proterozoic Athabasca Basin, Saskatchewan and Alberta*. Geological Survey of Canada, Bulletins, Ottawa, Canada, **588**, 23–67.

Johansson, A. 2009. Baltica, Amazonia and the SAMBA connection – 1000 million years of neighbourhood during the Proterozoic? *Precambrian Research*, **175**, 221–234.

Lazarov, M., Brey, G. P. & Weyer, S. 2009. Time steps of depletion and enrichment in the Kaapvaal Craton as recorded by subcalcic garnets from Finsch (SA). *Earth and Planetary Science Letters*, **279**, 1–10.

Leach, D. L., Bradley, D. C. *et al.* 2010. Sediment-hosted lead–zinc deposits in Earth history. *Economic Geology*, **105**, 639–659.

Li, Z.-X., Bogdanova, S. V. *et al.* 2008. Assembly, configuration, and break-up history of Rodinia: a synthesis. *Precambrian Research*, **160**, 179–210.

Li, Z.-X. & Zhong, S. 2009. Supercontinent-superplume coupling, true polar wander and plume mobility; plate dominance in whole mantle tectonics. *Physics of the Earth and Planetary Interiors*, **176**, 143–156.

Maier, W. D., Barnes, S. J., Sarkar, A., Ripley, E., Chusi, L. & Livesey, T. 2010. The Kabanga Ni sulfide deposit, Tanzania: I. Geology, petrography, silicate rock geochemistry, and sulfur and oxygen isotopes. *Mineralium Deposita*, **45**, 419.

Meert, J. G. 2002. Paleomagnetic evidence for a Paleo-Mesoproterozoic supercontinent 'Columbia'. *Gondwana Research*, **5**, 207–215.

Meert, J. G. 2012. What's in a name? The Columbia (Paleopangaea/Nuna) supercontinent. *Gondwana Research*, **21**, 987–993.

Mercadier, J., Cluney, M. *et al.* 2011. Origin of uranium deposits revealed by their rare earth element signature. *Terra Nova*, **23**, 264–269.

Meyer, C. 1981. Ore deposits as guides to geologic history of the Earth. *Annual Review of Earth and Planetary Science*, **16**, 147–171.

Mitchell, R. N., Kilian, T. M. & Evans, D. A. D. 2012. Supercontinent cycles and the calculation of absolute palaeolongitude in deep time. *Nature*, **482**, 208–212.

Naldrett, A. 2010. Secular variation of magmatic sulfide deposits and their source magmas. *Economic Geology*, **105**, 669–688.

Payne, J. L., Hand, M. *et al.* 2009. Correlations and reconstruction models for the 2500–1500 Ma evolution of the Mawson Continent. *In*: Reddy, S. M., Mazumder, R. R., Evans, D. A. D. & Collins, A. S. (eds) *Palaeoproterozoic Supercontinents and Global Evolution*. Geological Society, London, Special Publications, **323**, 319–355.

Pesonen, L. J., Elming, S.-Å. *et al.* 2003. Palaeomagnetic configuration of continents during the Proterozoic. *Tectonophysics*, **375**, 289–324.

Peterson, T. D., Pehrsson, S., Jefferson, C. & Scott, J. 2010. The Dubawnt Supergroup, Canada: a LIP with a LISP. International Association of Volcanology and Chemistry of the Earth's Interior – Large Igneous Provinces Commision; LIP of the Month, December.

Pisarevsky, S. A., Elming, S.-Å, Pesonen, L. J. & Li, Z.-X. 2014. Mesoproterozoic paleogeography: supercontinent and beyond. *Precambrian Research*, **244**, 207–225.

Reddy, S. M. & Evans, D. A. D. 2009. Palaeoproterozoic supercontinents and global evolution; correlations from core to atmosphere. *In*: Reddy, S., Mazumder, R., Evans, D. A. D. & Collins, A. S. (eds) *Palaeoproterozoic Supercontinents and Global Evolution*. Geological Society, London, Special Publications, **323**, 1–26.

Rogers, J. J. W. & Santosh, M. 2002. Supercontinents in Earth History. *Gondwana Research*, **6**, 357–368.

Wegener, A. 1912. Die Entestehung der kontinente. *Geologische Rundeschau*, **3**, 276–292.

Williams, S. E., Müller, R. D., Landgrebe, T. C. W. & Whittaker, J. M. 2012. An open-source software environment for visualizing and refining plate tectonic reconstructions using high-resolution geological and geophysical data sets. *GSA Today*, **22**, 4–9.

Xiaohui, Z., Qing, L., Yingjun, M. & Hui, W. 2005. Geology, fluid inclusions, isotope geochemistry, and geochronology of the Paishanlou shear zone-hosted gold deposit, North China Craton. *Ore Geology Reviews*, **26**, 325–348.

Zhang, S., Li, Z.-X. *et al.* 2012. Pre-Rodinia supercontinent Nuna shaping up: a global synthesis with new paleomagnetic results from North China. *Earth and Planetary Science Letters*, **353–354**, 145–155.

Zhao, G. C., Cawood, P. A., Wilde, S. A. & Sun, M. 2002. Review of global 2.1–1.8 Ga orogens: implications for a pre-Rodinia supercontinent. *Earth Science Reviews*, **59**, 125–162.